

## Supporting Information

### Experimental Section

#### Hydrothermal synthesis of vanadium pentoxide nanowires.

V<sub>2</sub>O<sub>5</sub> NWs were synthesized through a hydrothermal method as previously described<sup>1,2</sup>. VOSO<sub>4</sub>.nH<sub>2</sub>O (purity >99.9%), KBrO<sub>3</sub> (purity >98%), and nitric acid (purity ≥65%) were purchased from Alfa Aesar, Sigma Aldrich, and Trace SELECT® Ultra respectively. Briefly, 8 mmol of VOSO<sub>4</sub>.nH<sub>2</sub>O and 5 mmol of KBrO<sub>3</sub> were dissolved and stirred in 30 mL of Milli-Q water for about 30 mins at room temperature. Nitric acid was then added to the mixture solution dropwise until reaching pH of 1-2. Then the solution was transferred to a Teflon-lined stainless-steel autoclave for a reaction period of 24 h at 180 °C. The autoclave was cooled down to room temperature naturally before the solution was filtered and washed with Milli-Q followed by ethanol several times. The resulting green nanomaterial was dried at 80 °C under vacuum overnight.

#### Synthesis of V<sub>2</sub>O<sub>5</sub> NWs@DPA composite.

1 mg of V<sub>2</sub>O<sub>5</sub> NWs were added into 5 mL of 10 mM Tris-HCl buffer (pH 8.0) with the aid of homogenizer for about 2 mins. Then 3.2 µg of dopamine (DPA) were added into the homogeneous V<sub>2</sub>O<sub>5</sub> NWs solution and ultrasonicated for at least 2 hours to deposit DPA on the surface of the nanowire uniformly. The mixture was centrifuged at 10g for 30 mins and washed with Milli-Q water at least three times. The washing process would wash out any extra Tris-HCl buffer remaining in the mixture.

#### Synthesis of V<sub>2</sub>O<sub>5</sub> NWs@DPA@AuNPs cascade nanozyme.

1 mg of V<sub>2</sub>O<sub>5</sub> NWs@DPA was dispersed in 10 mL of Milli-Q water with the aid of homogenizer for about 3 mins. HAuCl<sub>4</sub> was added to reach the final concentration of 2 µM and ultrasonicated for 10 mins at room temperature. The freshly prepared NaBH<sub>4</sub> was added to reach the final concentration of 10 µM and further ultrasonicated for 15 mins at room temperature. The final mixture was then centrifuge at 10g for 30 mins and washed with Milli-Q water at least two times. The washing process would wash out free AuNPs in the solution.

To obtain the cascade catalytic activities, V<sub>2</sub>O<sub>5</sub> NWs@DPA composites 1, 2, and 3, containing 1.6 µg, 3.2 µg, and 6.4 µg DPA per 1 mg of V<sub>2</sub>O<sub>5</sub> NWs, respectively, were chosen to be decorated with AuNPs due to their high HPO-like activities (Fig. 1E). To obtain optimum GOx-like activity of AuNPs, we started with adding 100 µM AuNPs to the V<sub>2</sub>O<sub>5</sub> NWs@DPA composites (at the V<sub>2</sub>O<sub>5</sub> NWs concentration of 0.1 mg/ml), which we measured to provide about 2000 µM H<sub>2</sub>O<sub>2</sub> in one hour (Fig. S1). The V<sub>0</sub> of the HPO-like activity of V<sub>2</sub>O<sub>5</sub> NWs@DPA@AuNPs, using composites 1-3, was reduced by 41.0%, 44.5%, and 30.8% respectively in the presence of H<sub>2</sub>O<sub>2</sub> and Br<sup>-</sup>. It was reduced by 88.5%, 81.4%, and 82.3% respectively in the presence of glucose, O<sub>2</sub>, and Br<sup>-</sup> (Fig. S7A). We subsequently attempted to lower the concentration of AuNPs to 3 µM to a V<sub>2</sub>O<sub>5</sub> NWs@DPA solution with the V<sub>2</sub>O<sub>5</sub> NWs

concentration of 0.1 mg/ml, which we measured to provide 12  $\mu\text{M}$   $\text{H}_2\text{O}_2$  in one hour (Fig. S1). The  $V_0$  of the HPO-like activity of  $\text{V}_2\text{O}_5$  NWs@DPA@AuNPs, using composites 1-3, was reduced by 29.5%, 15.5%, and 22.3% in the presence of  $\text{H}_2\text{O}_2$  and  $\text{Br}^-$  and by 83.3%, 74.1%, and 77.6% in the presence of glucose,  $\text{O}_2$ , and  $\text{Br}^-$  (Fig. S7B). Therefore, lower concentrations of AuNPs led to greater cascade catalytic activities (likely due to less coverage of  $\text{V}_2\text{O}_5$  NWs active sites). The composites 2 showed the highest catalytic activity among all three tested and was thus used in further characterizations as described below.

The concentration of AuNPs in  $\text{V}_2\text{O}_5$  NWs@DPA@AuNPs was varied in the range of 1 – 3  $\mu\text{M}$  (in a  $\text{V}_2\text{O}_5$  NWs@DPA solution with the  $\text{V}_2\text{O}_5$  NWs concentration of 0.1 mg/ml) and characterized using the MCD method. The MCD results showed that  $\text{V}_2\text{O}_5$  NWs@DPA@AuNPs with 2  $\mu\text{M}$  AuNPs had the best catalytic activities (Fig. S8), with the  $V_0$  reduced by merely 2.27% in the presence of  $\text{H}_2\text{O}_2$  and  $\text{Br}^-$  and by 63.7% in the presence of glucose,  $\text{O}_2$ , and  $\text{Br}^-$  (Fig. S8), compared to  $\text{V}_2\text{O}_5$  NWs@DPA@AuNPs with 1 and 3  $\mu\text{M}$  AuNPs.

#### **Transmission electron microscopy (TEM) analysis.**

The TEM samples were prepared by dropping 5  $\mu\text{L}$  of nanowires/cascade nanozyme onto a holey-carbon coated copper grid for 10 s and suck the solution out using tissue. The low-magnification TEM and HRTEM images were acquired by using a field-emission-gun (FEG) FEI Tecnai F-20 microscope. Energy-dispersive X-ray spectroscopy (EDX) elemental mapping was obtained by using an Oxford X-Max detector. STEM-EDX mapping was set at a beam voltage of 200 keV and a pixel size of  $128 \times 128$ . Beam damage of STEM-EDX maps has been routinely observed before and after EDX mapping.

#### **X-ray photoelectron spectroscopy (XPS).**

Samples were analyzed using a Surface Science Instruments SSX-100 ESCA Spectrometer with operating pressure ca.  $1 \times 10^{-9}$  Torr. Monochromatic Al  $K\alpha$  x rays (1486.6 eV) with photoelectrons collected from an 800 $\mu\text{m}$  diameter analysis spot. Photoelectrons were collected at a  $55^\circ$  emission angle with source to analyzer angle of  $70^\circ$ . A hemispherical analyzer determined electron kinetic energy, using a pass energy of 150 eV for wide/survey scans, and 50 eV for high resolution scans. A flood gun was used for charge neutralization of non-conductive samples.

#### **Monochlorodimedone (MCD) method.**

The bromination activity was measured for 180 s at room temperature in Milli-Q water with 0.02 mg/mL  $\text{V}_2\text{O}_5$  NWs, 1 mM  $\text{Br}^-$ , 10  $\mu\text{M}$   $\text{H}_2\text{O}_2$ , and 50  $\mu\text{M}$  MCD ( $\epsilon_{290\text{nm}} = 19.1 \text{ mM}^{-1}\text{cm}^{-1}$ ). Potassium bromide (KBr) was used to provide  $\text{Br}^-$ . And the concentration of  $\text{H}_2\text{O}_2$  was calculated spectrophotometrically ( $\epsilon_{240\text{nm}} = 43.6 \text{ M}^{-1}\text{cm}^{-1}$ ).

$\text{V}_2\text{O}_5$  NWs and MCD were added to the mixture last, prior to the measurements to trigger the reaction. In order to measure the Michaelis-Menten kinetics, two independent sets of experiments were performed: 1)  $\text{Br}^-$  concentration was varied (0-20 mM) while keeping

concentrations of  $V_2O_5$  NWs/cascade nanozyme (0.02 mg/mL),  $H_2O_2$  (10  $\mu$ M) and MCD (50  $\mu$ M) constant. 2)  $H_2O_2$  or glucose concentration was varied (0-500  $\mu$ M) while keeping the concentration of  $V_2O_5$  NWs/cascade nanozyme (0.02 mg/mL), Br<sup>-</sup> (1 mM) and MCD (50  $\mu$ M) constant. For each measurement, blank tests and controls were performed, each measurement was carried out 4 times. The values were fitted to the Michaelis–Menten model and kinetic parameters were determined by Lineweaver–Burk linearization.

### **Detection of $H_2O_2$ production**

The rate of producing  $H_2O_2$  depending on the concentration of glucose in the range of 0-500 mM was measured with presence of 50  $\mu$ M AuNPs and injected air (providing  $O_2$ ) for one hour. The testing samples were then centrifuged at 10g for 2 mins. The suspension was tested using a  $H_2O_2$  fluorometric assay kit named Hydrogen Peroxide Assay Kit from Cayman Chemical. Briefly,  $H_2O_2$  was detected using 10-acetyl-3,7-dihydroxyphenoxazine (ADHP), a highly sensitive and stable probe for  $H_2O_2$ . In a horseradish peroxidase catalyzed reaction, ADHP reacts with  $H_2O_2$  with a 1:1 stoichiometry to produce highly fluorescent resorufin. The resorufin fluorescence can be detected using an excitation wavelength of 530 nm and an emission wavelength of 590 nm. The detected fluorescence was then compared with standard curve of  $H_2O_2$  to get exact amount of  $H_2O_2$  production.

### **Antimicrobial test.**

Non-typable Haemophiles influenza (NTHi) was cultured in a Brain Heart Infusion (BHI) medium with defibrinated horse blood and nicotinamide adenine dinucleotide (NADH) in a humidified 5%  $CO_2$ -containing balanced-air incubator at 37°C until the mid-log phase was reached, according to established protocols<sup>3</sup>. Then the suspension assay was used to determine the minimum inhibitory concentration (MIC) of nanowires/cascade nanozymes/ciprofloxacin for eradicating NTHi completely in 7 hours. The first formulation contained 0.04 mg/mL  $V_2O_5$  NWs, 1 mM Br<sup>-</sup>, and 20  $\mu$ M  $H_2O_2$ . The second formulation contained 0.04-0.16 mg/mL of  $V_2O_5$  NWs@DPA, 1 mM of Br<sup>-</sup>, and 20  $\mu$ M of  $H_2O_2$ . The third formulation contained 0.04-0.16 mg/mL of  $V_2O_5$  NWs@DPA@AuNPs, 1 mM of Br<sup>-</sup>, 62.5 mM of glucose with sustained air. The fourth formulation contained ciprofloxacin in the range of 0-0.8  $\mu$ g/mL. The optical density at 600 nm (OD600) was measured as a function of time using a microplate reader (Infinite M1000 Pro, Tecan). Background signals from nanowires/cascade nanozyme/ciprofloxacin were subtracted from the final reading. Subsequently, the MICs were confirmed by plating on chocolate agar plates after 7-hour incubation and kept in 37°C incubator with 5%  $CO_2$ .

### **Antibiofilm test.**

NTHi was cultured in a brain Hear Infusion (BHI) medium with defibrinated horse blood and nicotinamide adenine dinucleotide (NADH) in a humidified 5%  $CO_2$ -containing balanced-air incubator at 37°C until the mid-log phase was reached, according to established protocols<sup>3</sup>. Then the bacterial culture was diluted 10 times and 200  $\mu$ L of the diluted culture was pipetted into 96-well round bottom plates and incubated at 37°C with 5%  $CO_2$ . Media were carefully

replaced with 200  $\mu$ L of the fresh media daily. The cascade nanozymes and ciprofloxacin (at their respective MICs against planktonic NTHi) were used to treat NTHi biofilms after 3 days of growth. The treatment lasted for 24 hours under the same conditions as the aforementioned antimicrobial test. Growth of biofilm was then evaluated by crystal violet staining, Bactiter-Glo™ Microbial Viability Assay, and the LIVE/DEAD™ BacLight™ Bacterial Viability Kit. For crystal violet staining, biofilms were stained with 0.5 %wt crystal violet for 10 mins. Then excess crystal violet was removed by washing each well several times until the liquid in each well became a clear solution. The plates were air dried and stained biofilms dissolved by adding 30 v/v% acetic acid solution, which released the absorbed crystal violet for quantification. The total cell count in biofilms was analyzed spectrophotometrically by measuring the optical density at 570 nm (OD570, corresponding to the absorbance of crystal violet) using a microplate reader (Infinite M1000 Pro, Tecan). Background signals from nanowires/cascade nanozyme and plates were subtracted from the final reading.

Bactiter-Glo™ Microbial Viability Cell Assay provides a method to determine the number of live cells in a biofilm based on a quantification of ATP. The assay involves adding a single reagent (Bactiter-Glo™ Reagent) directly to bacterial cells cultured in medium and measuring luminescence. The luminescent signal is proportional to the amount of ATP and thus the number of live cells. Background signals from nanowires/cascade nanozyme and plates were subtracted from the final reading.

The LIVE/DEAD™ BacLight™ Bacterial Viability Kit was used to stain live and dead bacterial cells in a biofilm, and LSM710 Confocal microscope was used to take 2D and 3D images of the stained biofilms.

### **Cytotoxicity test in vitro.**

Human primary dermal fibroblasts (hFBs, ATCC PCS-201-012) were cultured and maintained in Fibroblast Basal Medium (FBM, ATCC PCS-201-020) with Fibroblast Growth Kit – Low Serum (ATCC, PCS-201-041) and 1% penicillin/streptomycin (Gibco) at 37°C with 5 % CO<sub>2</sub>. Once hFBs were seeded in sterile 96-well plates (Corning Costar) at a density of 10000 cells/well, the nanowires/cascade nanozymes formulations with 1 mM Br<sup>-</sup> and 10  $\mu$ M H<sub>2</sub>O<sub>2</sub> or 62.5 mM glucose with bubbling air were introduced into the cells and then incubated for 24 hours and 48 hours. CCK-8 kit for mammalian cells (Dojindo Molecular Technologies, Japan) was used to quantify the cell counts. Absorbance at 450 nm was measured after incubating cells with the CCK-8 kit reagents for 1–2 hours. Empty wells with CCK-8 assay reagents only were used as blanks and were subtracted from the final reading. Relative cell viability was calculated by normalizing the absorbance readings using that of nontreated cells. All assays were carried out in quadruplicates.

### **Statistical analysis.**

Data were analyzed using GraphPad Prism 7.0 software and presented as mean  $\pm$  SD. Student's t test or one-way ANOVA followed by Tukey's HSD test was applied for comparisons between two groups or among multiple groups.

## Figures

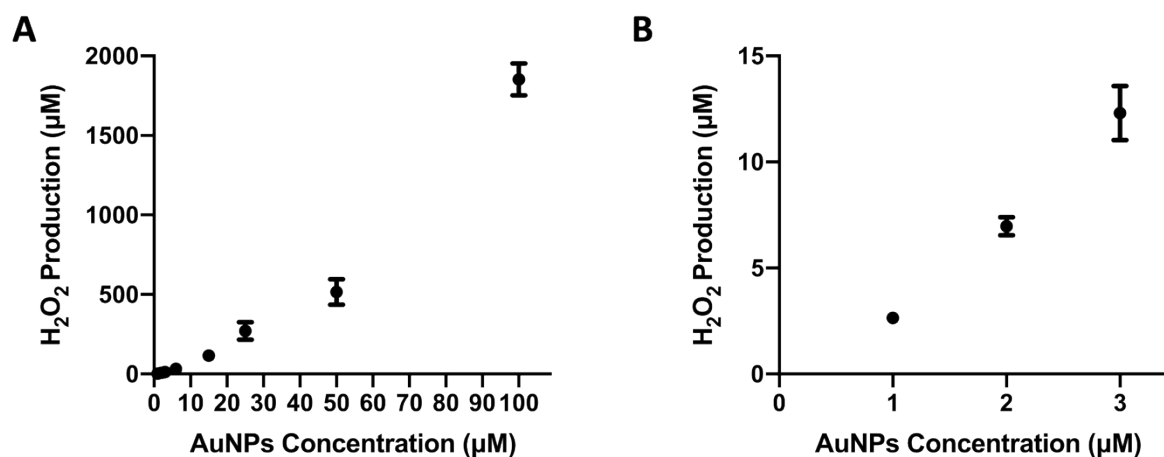


**Fig. S1. H<sub>2</sub>O<sub>2</sub> production based on different concentrations of AuNPs.** (A) The H<sub>2</sub>O<sub>2</sub> production as a function of AuNPs concentration (in range 0-100 µM), collected with 62.5 mM glucose and bubbling air. (B) The H<sub>2</sub>O<sub>2</sub> production as a function of AuNPs concentration (in range 1-3 µM) in (A), collected with 62.5 mM glucose and bubbling air. Data are mean ± SD. n=4.

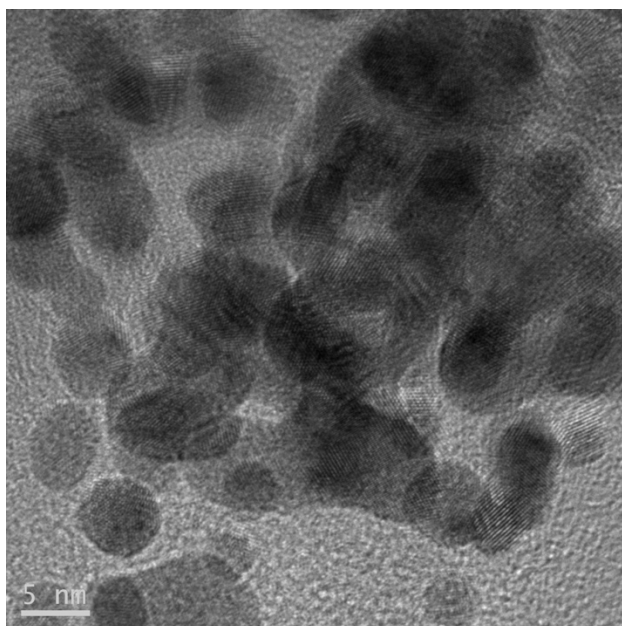


**Fig. S2. TEM image of naked AuNPs, showing unmodified AuNPs demonstrated a strong tendency to aggregate in solution.**

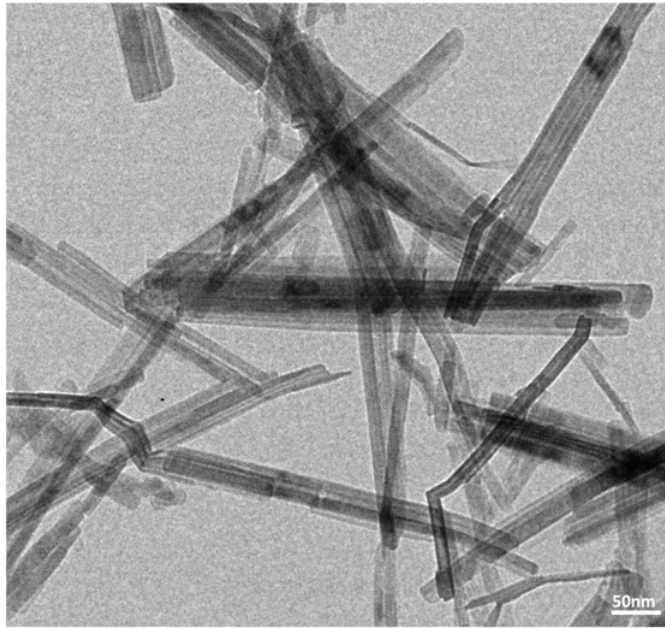


**Fig. S3. TEM of the V<sub>2</sub>O<sub>5</sub> NWs.**

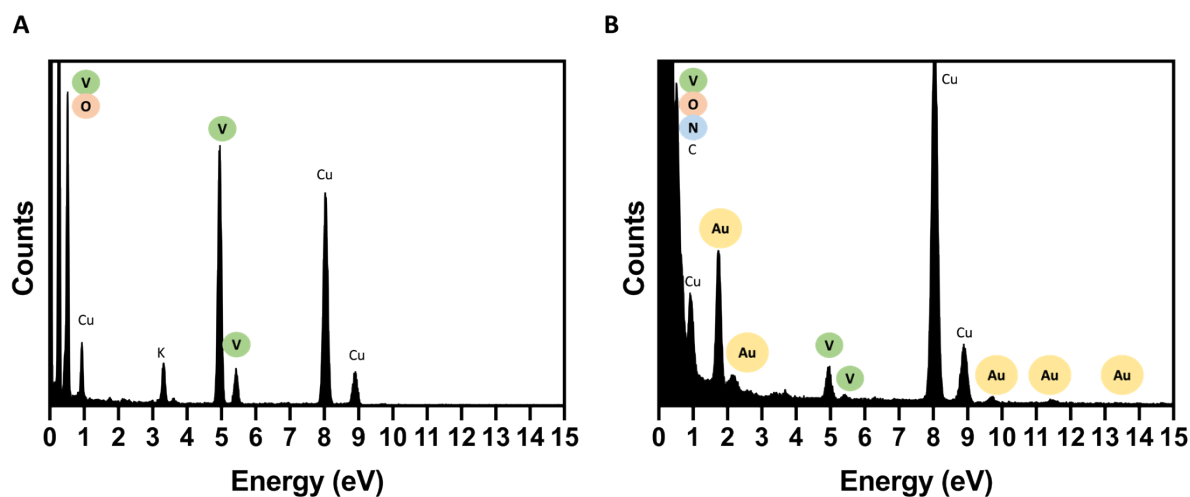


**Fig. S4. EDX spectrum of (A)  $V_2O_5$  NWs and (B)  $V_2O_5$  NWs@DPA@AuNPs cascade nanozyme.** The peaks of V (0.453, 0.511, 4.952, 5.427 eV), O (0.525 eV), N (0.392 eV), and Au (1.648, 2.123, 2.410, 8.494, 10.308, 11.443, 11.585, 13.710, 13.382 eV) were analyzed in EDX element mapping.

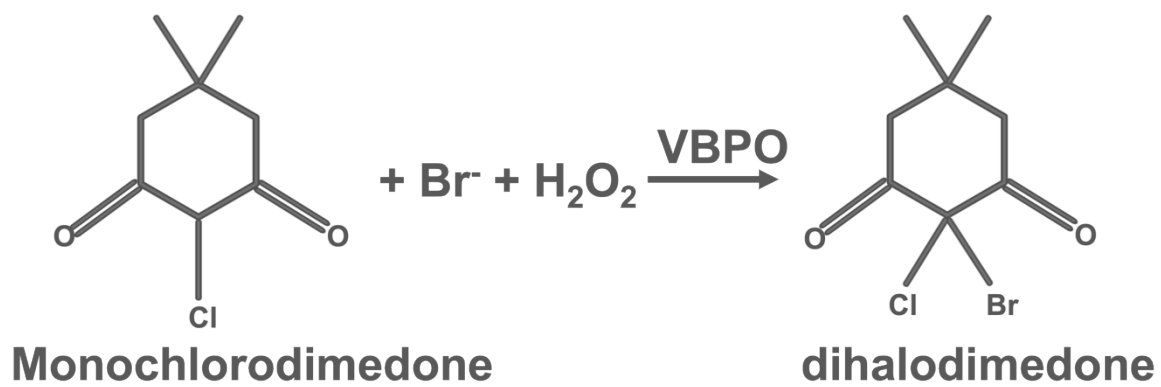


**Fig. S5. Scheme of the bromination of monochlorodimedone (MCD) to give dihalodimedone, used to quantify the reaction kinetics of HOBr generation.**

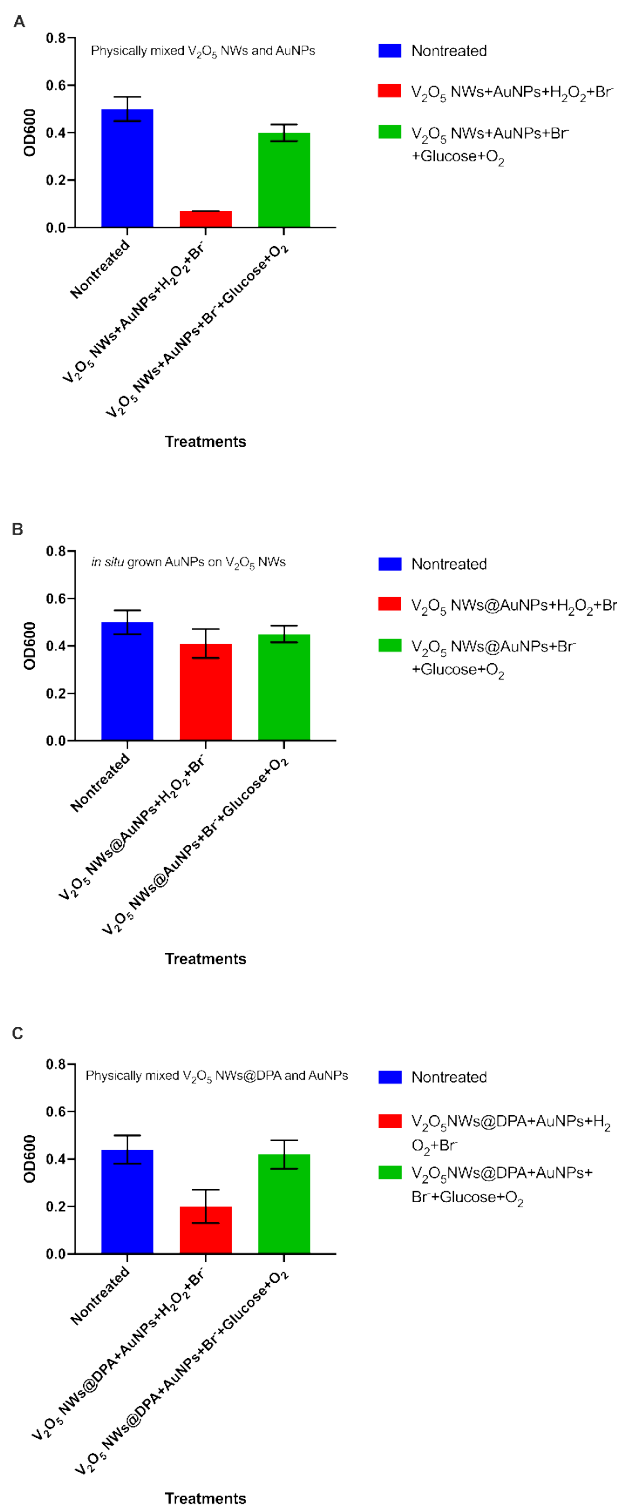


**Fig. S6. Antimicrobial effects of (A) physically mixed  $V_2O_5$  NWs and AuNPs, (B) *in situ* grown AuNPs on the surface of  $V_2O_5$  NWs, and (C) physically mixed  $V_2O_5$  NWs@DPA and AuNPs of NTHi. Data are mean  $\pm$  SD. n=4.**

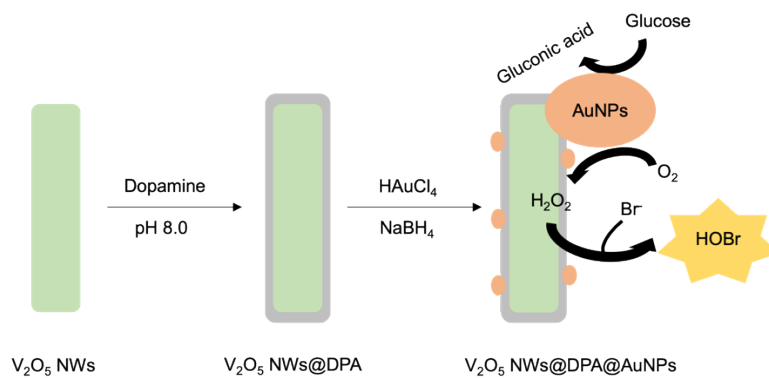


**Fig. S7. Scheme of the synthesis steps to obtain the cascade nanozyme.**

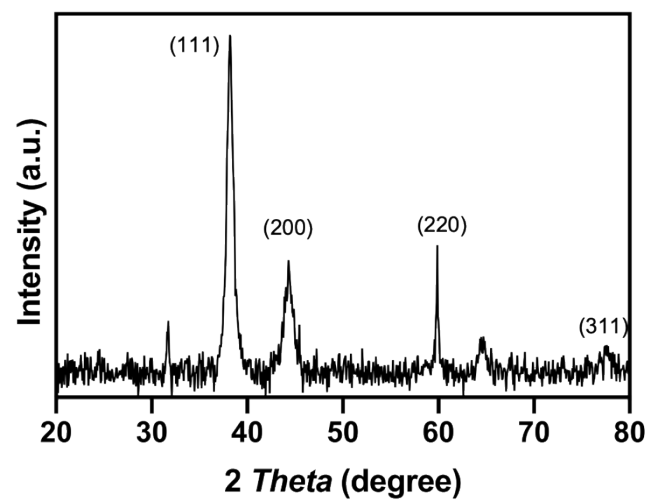


**Fig. S8.** XRD patterns of AuNPs

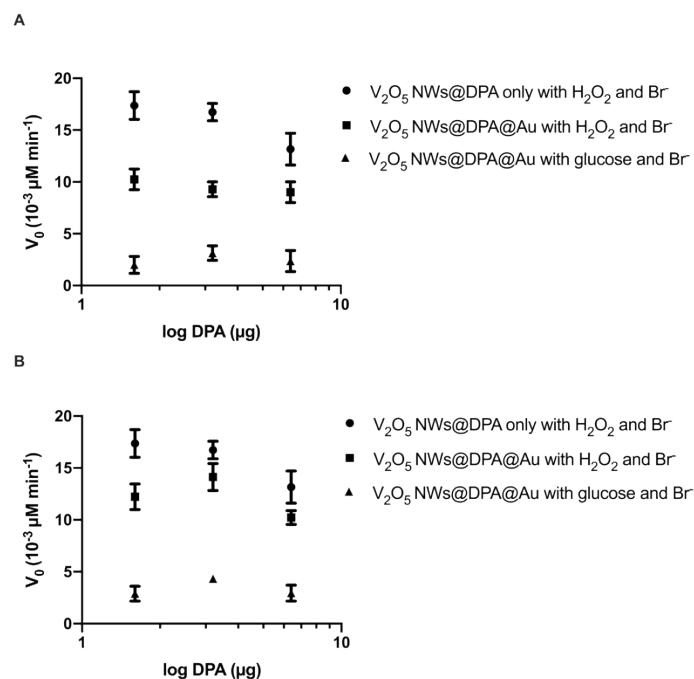


**Fig. S9. Catalytic activities of  $V_2O_5$  NWs @DPA@AuNPs with different concentrations of DPA and AuNPs.** (A) Solid circles represented the initial rate ( $V_0$ ) of  $V_2O_5$  NWs @DPA as a function of different DPA amount ( $\mu\text{g}$ ), and solid squares and triangles represented the  $V_0$  of  $V_2O_5$  NWs @DPA@AuNPs decorated with  $100 \mu\text{M}$  AuNPs as a function of different DPA amount ( $\mu\text{g}$ ), collected at the  $V_2O_5$  NWs @DPA /  $V_2O_5$  NWs @DPA@AuNPs concentration of  $0.02 \text{ mg/ml}$  (in terms of the weight concentration of  $V_2O_5$  NWs), the MCD concentration of  $50 \mu\text{M}$ , the  $\text{Br}^-$  concentration of  $1 \text{ mM}$ , and the  $\text{H}_2\text{O}_2$  concentration of  $10 \mu\text{M}$  or the glucose concentration of  $62.5 \text{ mM}$ . (B) Solid circles represented the  $V_0$  of  $V_2O_5$  NWs @DPA as a function of different DPA amount ( $\mu\text{g}$ ), and solid squares and triangles represented the  $V_0$  of  $V_2O_5$  NWs @DPA@AuNPs decorated with  $3 \mu\text{M}$  AuNPs as a function of different DPA amount ( $\mu\text{g}$ ), collected at the  $V_2O_5$  NWs @DPA /  $V_2O_5$  NWs @DPA@AuNPs concentration of  $0.02 \text{ mg/ml}$  (in terms of the weight concentration of  $V_2O_5$  NWs), the MCD concentration of  $50 \mu\text{M}$ , the  $\text{Br}^-$  concentration of  $1 \text{ mM}$ , and the  $\text{H}_2\text{O}_2$  concentration of  $10 \mu\text{M}$  or the glucose concentration of  $62.5 \text{ mM}$ . Data are mean  $\pm$  SD.  $n=4$ .

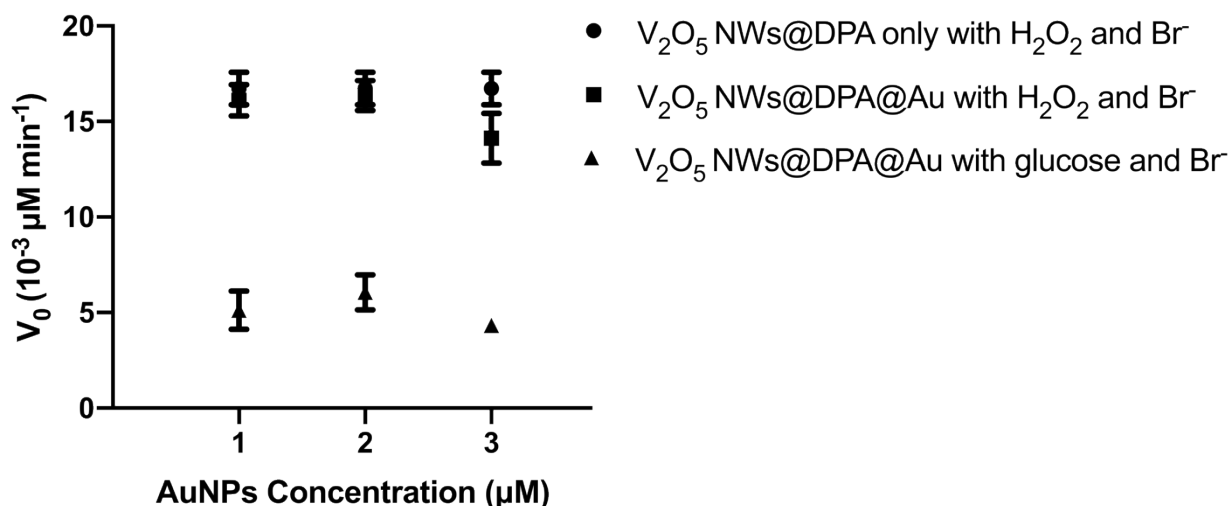


**Fig. S10. Catalytic activities of the composites 2 decorating with 1-3  $\mu\text{M}$  of AuNPs.** Solid circles represented the  $V_0$  of  $\text{V}_2\text{O}_5$  NWs @DPA, and solid squares and triangles represented the  $V_0$  of  $\text{V}_2\text{O}_5$  NWs @DPA@AuNPs as a function of different AuNPs concentration (1-3  $\mu\text{M}$ ), collected at the  $\text{V}_2\text{O}_5$  NWs @DPA / $\text{V}_2\text{O}_5$  NWs @DPA@AuNPs concentration of 0.02 mg/ml (in terms of the weight concentration of  $\text{V}_2\text{O}_5$  NWs), the MCD concentration of 50 $\mu\text{M}$ , the  $\text{Br}^-$  concentration of 1 mM, and the  $\text{H}_2\text{O}_2$  concentration of 10  $\mu\text{M}$  or the glucose concentration of 62.5 mM. Data are mean  $\pm$  SD. n=4.

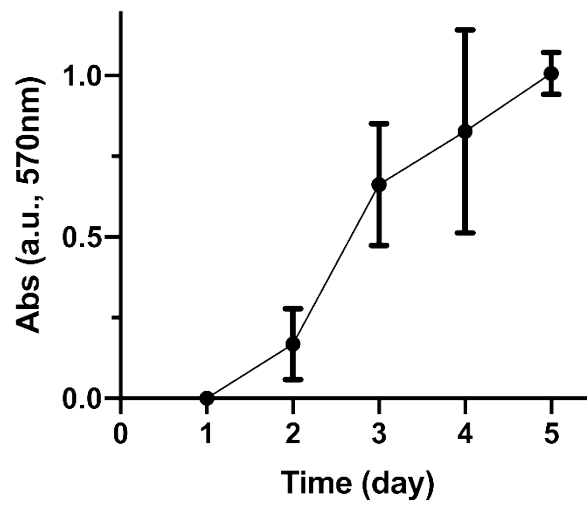


**Fig. S11.** NTHi biofilm growth curve. Data are mean  $\pm$  SD. n=5.

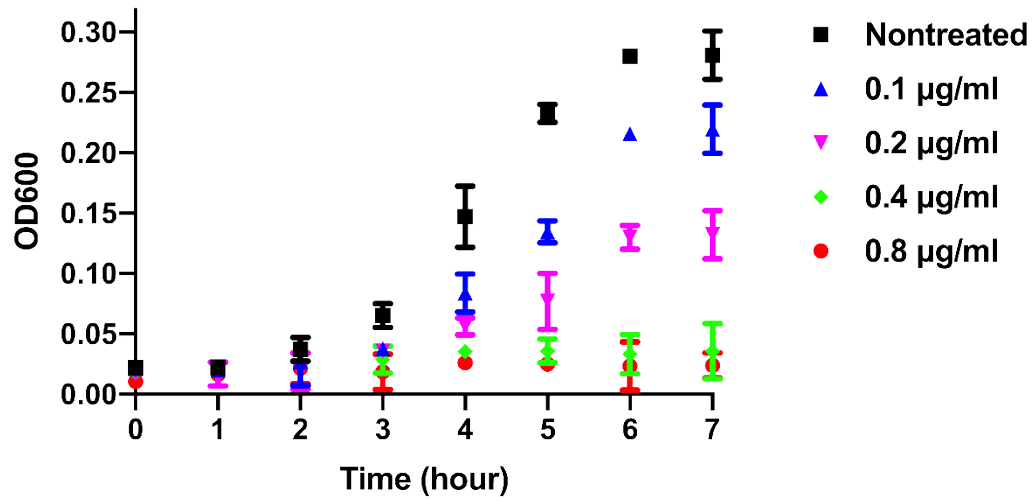


**Fig. S12. Antibacterial effect of ciprofloxacin on NTHi.** Minimum inhibitory concentration (MIC) was 0.4 µg/mL. Data are mean ± SD. n=4.

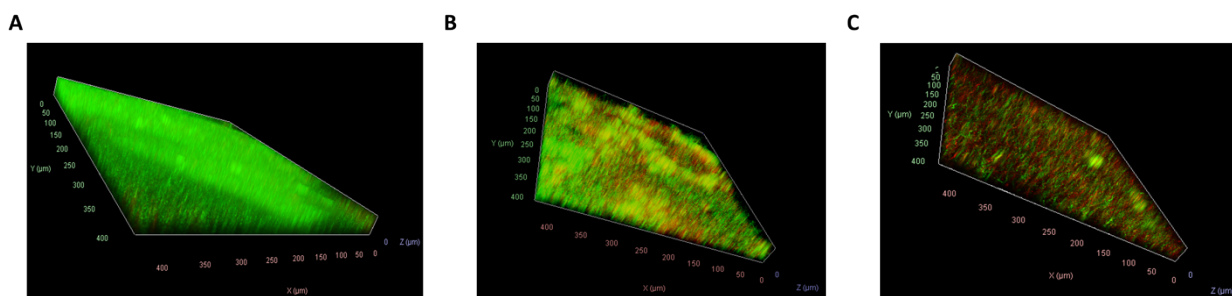


**Fig. S13. 3D Confocal images of nontreated and treated NTHi biofilm. (A)** nontreated NTHi biofilm, **(B)** NTHi biofilm treated with commercial antibiotic (ciprofloxacin), and **(C)** NTHi biofilm treated with  $V_2O_5$  NWs@DPA@AuNPs cascade nanozyme.

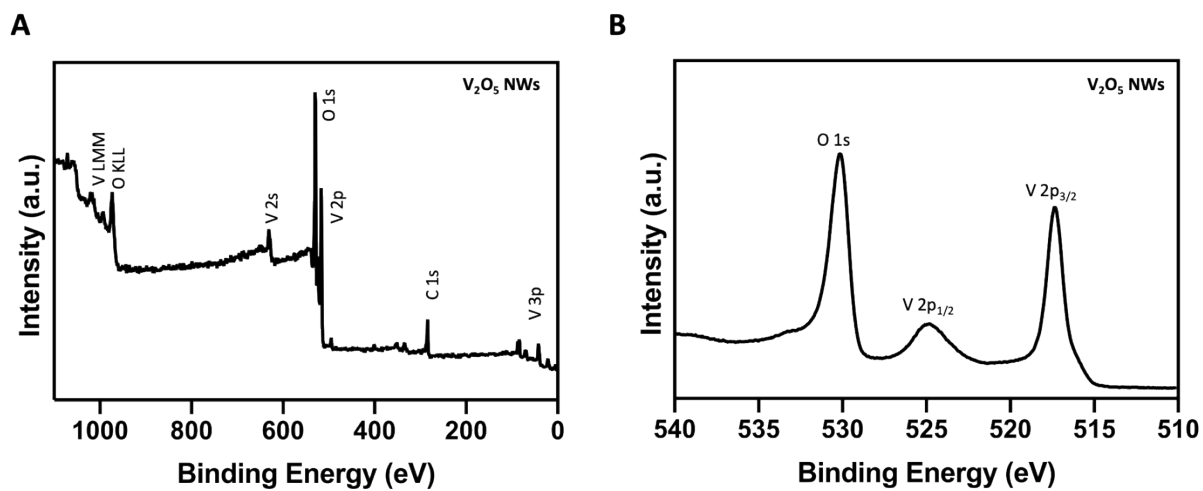


**Fig. S14. Characterization of  $V_2O_5$  NWs.** (A) XPS survey scan of the  $V_2O_5$  NWs. (B) High-resolution XPS spectra of the  $V_2O_5$  NWs in  $V_2O_5$  NWs.

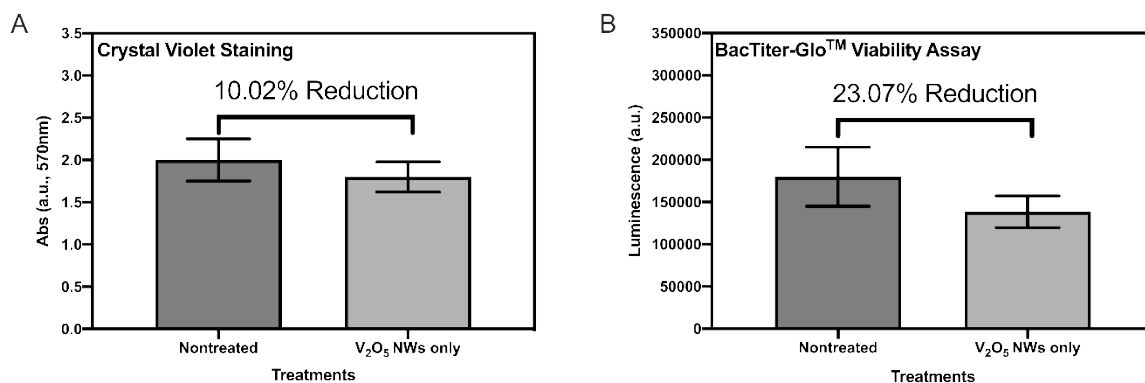


**Fig. S15. Antibiofilm effects of V<sub>2</sub>O<sub>5</sub> NWs.** NTHi biofilm was treated with 0.08 mg/ml V<sub>2</sub>O<sub>5</sub> NWs for 24 hours after three days of incubation. **(A)** Quantification of the crystal violet staining results of nontreated NTHi biofilm and NTHi biofilm treated with the 0.08 mg/ml V<sub>2</sub>O<sub>5</sub> NWs. **(B)** Quantification of the BacTiter-Glo™ Microbial Cell Viability Assay of nontreated NTHi biofilm and biofilm treated with the 0.08 mg/ml V<sub>2</sub>O<sub>5</sub> NWs. Data are mean ± SD. n=5.

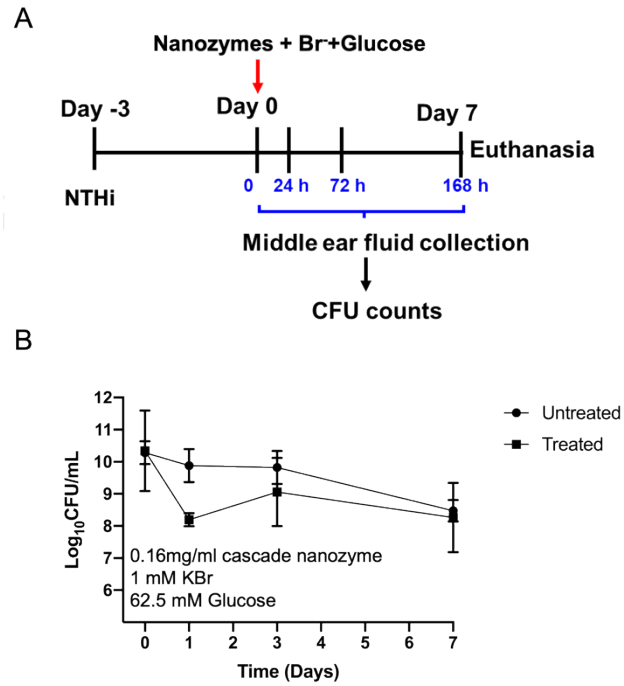


**Fig. S16. In vivo therapeutic efficacy of the cascade nanozyme in a chinchilla OM model.** (A) The timeline of the in vivo procedures to induce and treat OM in chinchillas. (B) Time course of the bacterial CFU count in the MEF of animals with OM. The formulations contained 0.16 mg/mL cascade nanozyme, 1 mM Br<sup>-</sup>, and 62.5 mM glucose. Data are mean ± SD. n=3.

**TABLES**

**Table S1. Kinetic parameters of different haloperoxidases.**

<b>Catalyst</b>	<b>Substrate</b>	<b>K<sub>m</sub> (M)</b>	<b>V<sub>max</sub> (M s<sup>-1</sup>)</b>	<b>Reference</b>
V <sub>2</sub> O <sub>5</sub> NWs	Br <sup>-</sup>	0.25 × 10 <sup>-3</sup>	5.17 × 10 <sup>-10</sup>	This work
	H <sub>2</sub> O <sub>2</sub>	10.26 × 10 <sup>-6</sup>	7.26 × 10 <sup>-10</sup>	
V <sub>2</sub> O <sub>5</sub> NWs	Br <sup>-</sup>	0.2 × 10 <sup>-3</sup> (Tris-HCl) 0.6 × 10 <sup>-3</sup> (PBS)	7.3 × 10 <sup>-10</sup>	F. Natalio et al., Nature Nano., 2012. <sup>1</sup>
	H <sub>2</sub> O <sub>2</sub>	10 × 10 <sup>-6</sup> (Tris-HCl) 10 × 10 <sup>-6</sup> (PBS)	7.3 × 10 <sup>-10</sup>	
Vanadium chloroperoxidase (V-CPO) from <i>C. inaequalis</i>	Br <sup>-</sup>	3.1 × 10 <sup>-3</sup>		Z. Hasan, et al., J. Biol. Chem. 2006. <sup>4</sup>
	H <sub>2</sub> O <sub>2</sub>	16 × 10 <sup>-6</sup>		
Vanadium bromoperoxidase (V-BPO) from <i>A. nodosum</i>	Br <sup>-</sup>	18.1 × 10 <sup>-3</sup>		E. de Boer, J. Biol. Chem. 1988. <sup>5</sup>
	H <sub>2</sub> O <sub>2</sub>	22 × 10 <sup>-6</sup>		

## References

- 1 F. Natalio, R. André, A. F. Hartog, B. Stoll, K. P. Jochum, R. Wever and W. Tremel, *Nat. Nanotechnol.*, 2012, **7**, 530–535.
- 2 F. Zhou, X. Zhao, C. Yuan and L. Li, *Cryst. Growth Des.*, 2008, **8**, 723–727.
- 3 X. Ma, J. Lang, P. Chen and R. Yang, *AIChE J.*, 2021, 1–14.
- 4 Z. Hasan, R. Renirie, R. Kerkman, H. J. Ruijssenaars, A. F. Hartog and R. Wever, *J. Biol. Chem.*, 2006, **281**, 9738–9744.
- 5 E. de Boer and R. Wever, *J. Biol. Chem.*, 1988, **263**, 12326–12332.